Saha *et al. Environ Syst Res (2016) 5:4*
DOI 10.1186/s40068-016-0057-2

Environmental Systems Research
a SpringerOpen Journal

RESEARCH

Open Access

A combined numerical and neural technique for short term prediction of ocean currents in the Indian Ocean

Dauji Saha[1], M. C. Deo[1*], Sudheer Joseph[2] and Kapilesh Bhargava[3]

Abstract

Background: Short term current prediction for operational purposes is commonly carried out with the help of numericalocean circulation models. The numerical models have advantage that they are based on the physics of the underlying process. However because of their spatial nature they may not be so accurate while making station-specific predictions. In such cases data-driven approaches like artificial neural network (ANN)'s trained on the basis of location-specific data may work better. In this paper an attempt is made to do daily predictions of ocean currents by combination of a numerical model and ANNs.

Results: The difference in the current velocity estimated by the numerical model and actual observations at a given-time was calculated and corresponding error time series was formed based on all past numerical estimations and observations. An ANN was trained over such time series to predict errors for future, which were added to the numerical estimation so as to predict daily current velocities over multiple days in future.

Conclusions: The suggested approach, implemented at two locations in Indian Ocean, was found to perform satisfactory current predictions up to a lead time of 5 days, as ascertained through various error statistics. The standalone networks once trained using the numerical outcome can reproduce such output well over future time without using variety of data and computational resources required for running the numerical model on a continuous basis.

Keywords: Numerical current models, Artificial neural network, Current prediction, Ocean currents, Current observations

Background

The operational prediction of ocean currents is necessary for carrying out a variety of activities such as shipping and towing as well as search and rescue, tracking pollutants and oil spill, monitoring coastal water quality, forecasting power output from current energy farms, and, issuing warnings to fishermen and to organizers of sports and swimming events. Presently methods of predicting currents are based on numerical modeling in which the governing differential equations are solved using a suitable numerical procedure. The numerical models are essentially targeted toward spatial predictions at a given time and hence may face limitations arising out of modeling assumptions, incompleteness of boundary conditions and forcing functions, large computing requirements and may need local tuning.

The performance of a numerical current model can be enhanced by various means. It can be done in time-independent or offline mode as in the optimal interpolation approach or in time-dependent or online mode as in variational methods and Kalman Filter. The underlying schemes incorporate an update of (i) input parameters, (ii) state variables, (iii) model parameters, and (iv) output parameters. The last approach has advantages like simplicity, less requirement of data in general and it is suitable for site-specific predictions (Jain and Deo 2006).

Some of the recent studies dealing with current prediction using physics based methods are given below:

*Correspondence: mcdeo@civil.iitb.ac.in
[1] Department of Civil Engineering, Indian Institute of Technology Bombay, Mumbai, India
Full list of author information is available at the end of the article

Farrara et al. (2013) developed a three-dimensional ocean model based on ROMS driven by output from a regional atmospheric model component and validated against independent observations. The vertical current profile matched well with the moored ADCPs and the surface currents were in good agreement with the drifter trajectories, thus confirming that the evolution of the surface flow was captured well in the model.

A real-time ocean prediction system for the Western North Atlantic was developed by Schimdt and Gangopadhyay (2013) for the Mid-Atlantic Regional Association Coastal Ocean Observing System based on the physical circulation model component of the Harvard Ocean Prediction System (HOPS), which captured the mesoscale dynamics of the Gulf Stream, its meanders and rings, and its interaction with the shelf circulation, the mid-Atlantic shelf, and the buoyancy-driven circulation in the Gulf of Maine. The model showed reasonable skill in simulating currents, especially over days 1–3 of simulation.

In order to assess the model sensitivity to the parameterization of different processes and implementation strategies, Bolanos et al. (2014) employed the 'MIKE 3/21' modelling system, together with measurements of wind, waves, currents and water levels at one location, and used the same to investigate the currents dynamics of the northern Adriatic basin. Depth-averaged, surface and bottom currents were more difficult to reproduce and the observed high variability was not fully captured by the model systems possibly due to reasons like model configuration, spatial resolution and probably inadequate modeling of sub-processes, like, atmosphere–ocean momentum, heat transfers, and, turbulence.

Located between the South China Sea and Andaman Sea, the hydrodynamics in Singapore Strait is driven by tides coming from both sides and thus is complex. In order to overcome the limitations in predicted water levels and currents due to parametric uncertainty, forcing and lateral boundary conditions Karri et al. (2014) employed a data assimilation technique based on ensemble Kalman filter with good results.

Rahaman et al. (2014) combined the National Oceanic and Atmospheric Administration (NOAA) Geophysical Fluid Dynamics Laboratory's Modular Ocean Model (MOM4p1) (run at global climate model resolution of 1^0) and a regional Indian Ocean MOM4p1 configuration (with 25 km horizontal resolution and 1 m vertical resolution near the surface). This along with consideration of with the use of realistic topography and seasonal river runoff helped in better predictions of observed currents in Indian Ocean.

Kowalik et al. (2015) compared the tides and currents obtained from numerical model in the western fjords of Svalbard with observations (measured sea levels and drifters) and inferred that the tidal amplitude did not change strongly in these fjords but the tidal currents were enhanced in several locations.

An ocean forecast system for the South China Sea was developed by Wang et al. (2015) using a multi-grid regional ocean circulation model that was established on the basis of ROMS. In order to improve on the results authors incorporated wave induced vertical mixing along with a data assimilation procedure.

In India the Indian National Centre for Ocean Information Services (INCOIS) located at Hyderabad has a hybrid coordinate type model which provides operational current forecasts (http://www.incois.org). The current simulations are based on a 3-D global ocean circulation model called: hybrid coordinate ocean model (HYCOM) (http://www.hycom.org*)*. In such a model the ocean circulation is conceptualized into differential equations of mass continuity, momentum and advection–diffusion and solved using finite difference schemes.

In the present work we first evaluate the accuracy of current velocities estimated by the model: HYCOM with respect to actual current measurements made at two sites in the Indian Ocean and thereafter predict values of daily current velocities over 5 days in advance using an artificial neural network (ANN). The resulting approach will have advantage of both physically based and data driven techniques.

The purpose of this work is to check first if the HYCOM output that is based on a numerical method is accurate enough at a particular station or location. The need to do so arises from the fact that the numerical methods are essentially targeted to obtaining information over a large spatial domain rather than at a specific station, which is required typically in applications such as engineering operations and design. The accuracy of the results of numerical model is checked by comparing them with the actual measurements and thereafter improved using an ANN. The usefulness of ANN vis-à-vis traditional statistical or numerical methods has been demonstrated in a number of studies in the past (as summarized in Jain and Deo 2006). Their relative advantage is due to their ability to make estimations or predictions without assumption of any mathematical model a priori, as well as lack of requirement of any exogenous data, and, inherent tolerance to errors.

Alternatively an ANN can be trained using location-specific measurements and used for forecasting, (as done in Charhate et al. 2007) such an approach based entirely on data-driven schemes has not received wide acceptance from the user community who traditionally believes in the physics-based approach. We have therefore tried to combine both numerical as well as data driven techniques in this work.

In case of site specific predictions it may be noted that the problem of downscaling a global low-resolution general circulation models to the regional high-resolution scale has been addressed in the past through methods like regression, weather pattern matching, limited area models and stochastic weather generators (Wilby and Wigley 1997). However these approaches are more suitable for climate modelling involving long term predictions, unlike the present case of short term station-specific forecasting. For short term current predictions the normal procedure is to run a numerical model over a future time step on the basis of forcing of causal variables such as wind and tide over a future time step.

In our study the error between the numerical estimation and corresponding observation at a given time step was calculated and an error time series was thus formed based on records of historical numerical values and corresponding measurements. An ANN was thereafter used to carry out 'time series forecasting' and the errors were forecasted over multiple time steps in future. These were added to the numerical estimation and predictions of current velocities over desired time steps in future were made. The 'addition' of error here indicates combining the error with the numerical estimation with appropriate sign. The sampling interval used in this work was daily (mean) and predictions were made over a time horizon of next 5 days.

It may be noted that studies made by a large number of researchers worldwide have shown effectiveness of ANN's in time series forecasting and wave analysis (Londhe and Panchang 2006, and, Makarynskyy 2004). An overview of ANN applications in ocean engineering in general has been given in (Jain and Deo 2006). In particular Charhate et al. (2007) have shown how ANN's can effectively carry out short term current forecasting in a tide dominated bay based on real time current measurements made at a specific site. Similarly Saha et al. (2015) have demonstrated how efficiently trained networks can overcome certain deficiencies of such ANN methods.

ANN's basically map a given random vector of inputs (preceding sequence of errors in the numerical current estimation, in our case) with corresponding one of outputs (predicted error over subsequent time steps) without necessity of involving physics of the process or causal variables. Hence the ANN in our study does not require any meteorological, oceanographic or morphological forcing.

In order to improve on the numerical outcome data assimilation is common. Toward this alternative schemes such as updating input, updating model parameters or updating state variables through stochastic methods are employed (Sannasiraj et al. 2006). It is known that such data assimilation involves rerunning entire numerical model with high computational effort. Instead we are proposing here a simpler and straight forward post-processing scheme of combining the ANN predicted errors with the numerical outcome. While it is true that such errors can also be predicted by other time series prediction methods like AR, ARMA, and ARIMA, it has been widely reported in the past works (as reviewed in Jain and Deo 2006, mentioned in the manuscript) that the 'model-free' soft computing methods like ANN normally work much better than the 'model based' statistical methods. In order to have a sustainable approach, that should be valid at any location in general, we have thus employed the ANN only.

The numerical current model

The governing equations in the numerical HYCOM model are as follows:

Continuity equation:

$$\frac{\partial}{\partial t}\Delta p_{\mathrm{k}} + \nabla(\mathbf{u}\Delta p)_{\mathrm{k}} = 0; \tag{1}$$

where, t = time; Δp = thickness of the vertical depth layer 'k'; $\mathbf{u}$ = horizontal velocity;

Momentum equation:

$$\frac{\partial u}{\partial t} + \nabla\frac{\mathbf{u}^2}{2} + (\zeta + f)\boldsymbol{k}\times\mathbf{u} = -\nabla M - g\frac{\partial\tau}{\partial p} \tag{2}$$

where, ∇ = spatial operator, operating on isopycnal surface; ζ = relative vorticity; f = Coriolis parameter; $\boldsymbol{k}$ = vertical unit vector; M = Montogomery potential; g = acceleration due to gravity; τ = Reynold's stress; Δp = change in thickness;

Advection–diffusion:

$$\begin{aligned}&\frac{\partial}{\partial t}T\Delta p + \nabla\cdot(\mathbf{u}T\Delta p) + \left(\dot{S}\frac{\partial p}{\partial s}T\right)_{bot}\\&\quad - \left(\dot{S}\frac{\partial p}{\partial s}T\right)_{top} = \nabla\cdot(\vartheta\Delta p\nabla T) + H_T\end{aligned} \tag{3}$$

where, T = temperature (of a layer 'k')' $\dot{\boldsymbol{S}}\frac{\partial p}{\partial s}$ = vertical mass flux; suffix 'bot' refers to bottom; suffix 'top' refers to top; H_T = radiative exchanges.

The specialty of HYCOM is that it uses the density-following or isopycnic coordinates in an open stratified sea and terrain-following ones in un-stratified or coastal region and thus can retain characteristics of water mass for long time duration. Also, the grid coordinates are thus controlled in a very efficient manner. HYCOM also satisfactorily represents thermodynamics of the ocean through high vertical resolutions. Compared with alternatives HYCOM has better system design, finer horizontal and vertical resolutions and smoother transition from deep to shallow water (Joseph and Ravichandran, 2013).

HYCOM is configured for the Indian Ocean with longitudinal limits of 20°–125° E and latitudinal limits of 35° S–31° N. The model adopts boundary conditions from global HYCOM simulations at the eastern, southern and south-eastern boundaries. It has around 25 km horizontal resolution at mid-latitudes and it encompasses 28 vertical layers. Presently the model is run in a non-assimilation model.

Data used

The numerical model HYCOM was run over the Indian Ocean with spatial resolution of (1/4) degrees and data pertaining to two horizontal components of current were extracted at two locations (site: 1 and site: 2, Fig. 1) for the same duration for which the actual measurements at these sites were available. This duration was around 30 months (November 4, 2009–April 1, 2012) at site 1 and 24 months (May 18, 2010–Apr. 2, 2012) at site 2. The coordinates of these deep water sites: 1 and 2 are 8° N and 90° E, and 12° S and 80.5° E, respectively. These locations were identified by considering absence of gaps and quality of both types of data during the sampling period.

Site 1 is near the equator and in the northern Indian Ocean. At this location variability in the zonal velocity, within and across different seasons, is largely influenced by generation and propagation of long waves (Fu 2007; Iskandar and McPhaden 2011). The southern site 2 is located near the eastern edge of the thermocline ridge and the flow of currents here is more likely to be influenced by the Rossby waves moving slowly away from the equator (Hermes and Reason 2008; Masumoto and Meyers 1998) and also by the eddies at the mid-latitudes (Chelton et al. 2011). Thus variability of current in time and space at the two locations could be very different.

Detailed discussion on the applicability of the present approach would call for consideration of many locations than the two. However availability of simultaneous numerical and observed data at multiple locations was constraint in this work.

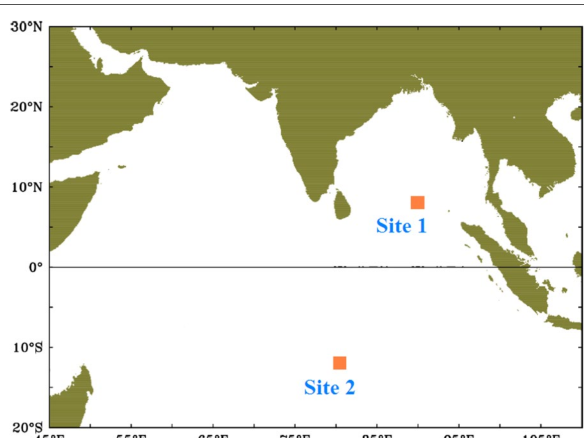

Fig. 1 The site 1 and site 2 of the study (Source: Joseph and Ravichandran 2013)

The current measurements were made as part of a project nicknamed: RAMA (derived from: Research Moored Array for African-Asian Australian Monsoon Analysis and Prediction), which is a multinational effort to provide real time data for climate research and forecasting. The major components of this international exercise include the buoy array: TAO/TRITON in the Pacific, PIRATA in the Atlantic, and RAMA in the Indian Ocean (http://www.pmel.noaa.gov/tao/proj_over/proj_over/). The currents were observed at 10 m depth by a Sontek Current Meter. Its resolution was 0.1 cm/s for the speed and 0.1° for the direction. The range of the measurements was 0–600 cm/s and the accuracy was ± 5 cm/s for speed and ± 5° for direction (McPhaden et al. 2009).

(http://www.pmel.noaa.gov/tao/data_deliv/)

A pictorial representation of observed current data is given in Fig. 2a, b through rose diagrams. Figure 2a pertains to site 1 and Fig. 2b to site 2. These rose diagrams show the current distribution over the entire time period under consideration. The velocities were grouped into 36 directions at 10° intervals. The concentric circles show the frequency of occurrence varying from 0 to 6 % at site 1 and 0–11 % at site 2. Along each direction different colors show different ranges of the speed varying from 0 to 80 cm/s.

Figure 2a indicates that at site 1 the current speeds were up to 80 cm/s and mostly spread, whereas at site 2 (Fig. 2b) the currents were relatively more focused in their direction of propagation and this was mostly toward west to south–west, with speeds less than 80 cm/s.

The methodology

The ANN's developed for preparing the error time series were of uni-variate auto-regressive type in which a sequence of preceding observations was fed to the network every time, enabling it to guess an unknown pattern in it and move ahead to predict the value at the next time step, consistent with the same pattern, every time in a sliding window fashion.

It was found through experimentation that a feed-forward back-propagation type ANN (Fig. 3) worked well for this application, in comparison with some other complex architecture such as radial basis and generalized regression. Such a network consisted of three layers of computational elements or neurons. The input is fed into the network through the input layer while the output is collected from the output layer. The neurons in the hidden layer bring in required non-linearity in the system. Initially the connection weights (shown by dots across the linkages) as well as the bias are equated to random

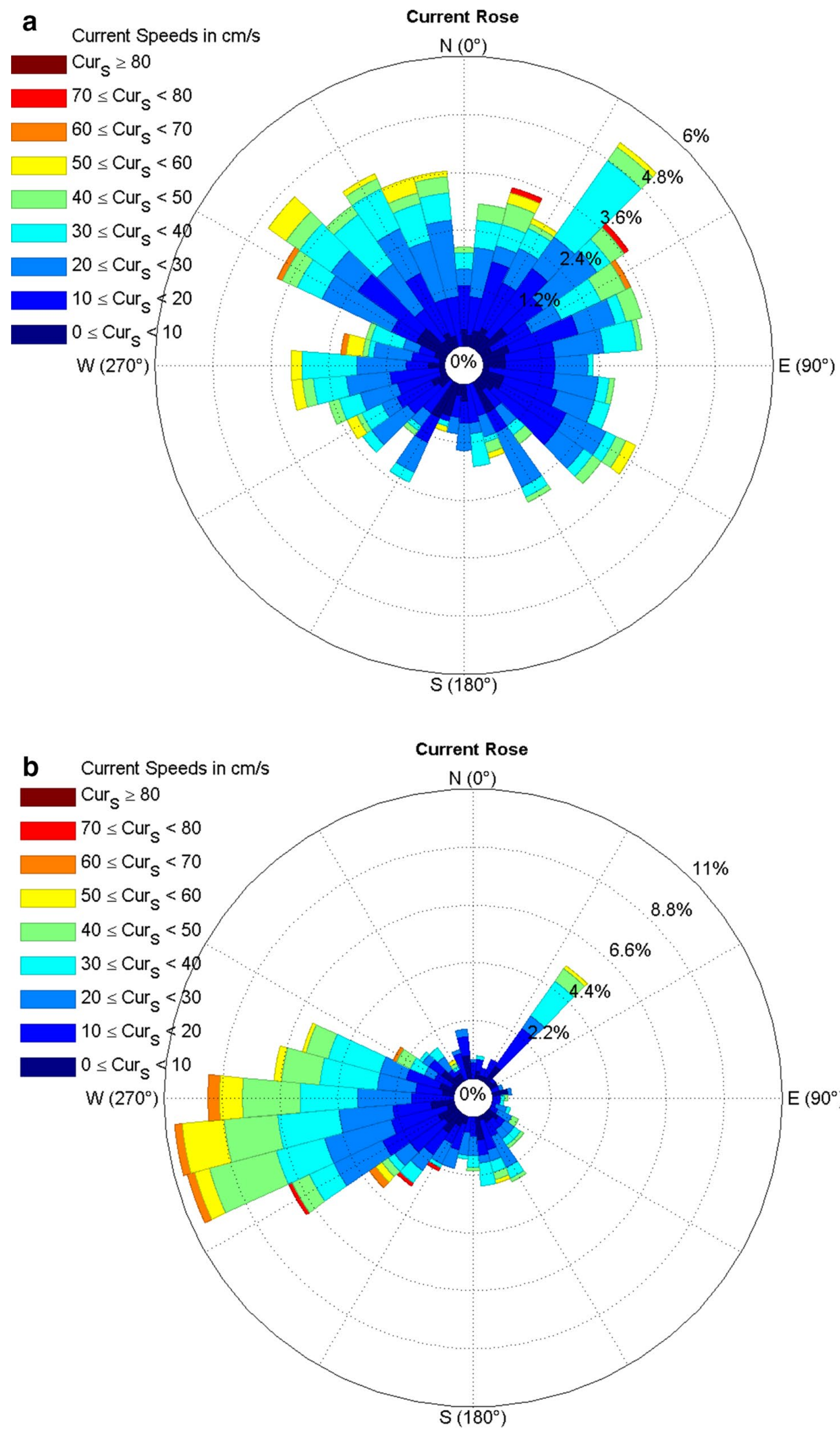

Fig. 2 Observed current rose diagrams at site 1 (**a**) and 2 (**b**)

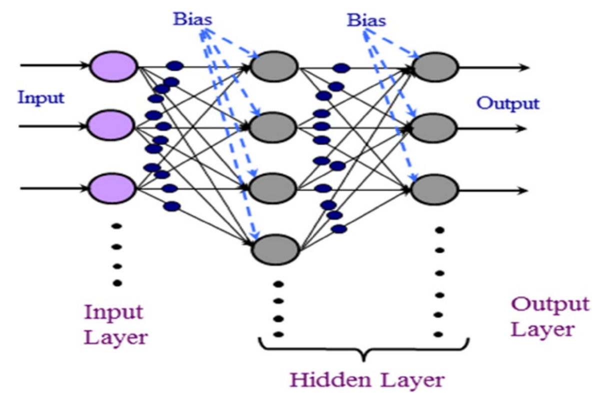

Fig. 3 The neural network used

numbers and their final values are determined iteratively through a training algorithm and by feeding known input–output pairs one after the other. In this work it was found that the algorithm of resilient back-propagation that carries out the descent of error (or the difference between the target output and the realized one) gradient adaptively yielded desired results (Wasserman 1993, Wu 1994 and Sivakumar and Berndtsson 2010).

Each hidden neuron collects a weighted input from all linked neurons, adds a bias term to it and passes on the summation through a transfer function. The result of this operation is sent to neurons in the subsequent output layer. The transformed output from the output neuron/s is the final outcome from a network.

The input to our ANN consisted of a segment of past values of the errors. The length of the segment (or the number of neurons in the input layer, say, 5) was ascertained by experiments aimed at achieving the best performance. The output was the predicted error corresponding to the lead time under consideration. For each lead time separate networks were developed. The number of hidden nodes was selected through trials aimed at obtaining the best testing performance and this was typically 10. The training algorithm of resilient back-propagation referred to earlier involved the use of a momentum factor of 0.7 and learning rate of 0.9

The total amount of data was divided into two sets: training (or calibration) and testing. The first 70 % of data segment was used for training while the remaining one was employed for testing.

As mentioned earlier the error time series was first formed by getting the error between the numerical estimation and corresponding observation at the current time step. The network thereafter carried out the time series forecasting and predicted errors over multiple time steps in future, which were added to the numerical estimation and predictions of currents over desired time steps in future were produced.

Results

Accuracy of the numerical model

To begin with, the prediction accuracy of the numerical model at the two selected locations was studied. For this purpose the difference between the numerical outcome and corresponding actual measurement (daily mean values) was evaluated over the entire sample size through the error statistics of correlation coefficient, R, root mean square, RMSE, and mean absolute error, MAE. The correlation coefficient, R, indicates the degree of linear association between predicted and target values. It is sensitive to outliers but insensitive to proportional or additive differences. The RMSE is an error index giving an overall error picture, although sensitive to extreme values due to square of the differences involved. The MAE gives an estimate of accuracy of the overall prediction at the absolute scale. As each error measure has usefulness as well as limitations multiple statistics have been evaluated.

The above mentioned statistics are shown in Table 1 that provides separate performance over the northward (or meridional or V-) component and the eastward (or zonal or U-) component. For both locations the R values were low and the RMSE and MAE statistics were high. The worst prediction was that of the meridional (northward) velocity component. It was therefore thought worthy to see if supplementation of the numerical model by a data-driven scheme can be beneficial in making site-specific current predictions.

Site 1

As an example the error time series at this location over the testing duration of November 4, 2009–April 1, 2012 is shown in Fig. 4 with respect to both u- and v-components separately. The ANN operated on such time series. The ANN architecture as well as control parameters have been given earlier in "The methodology" Section.

The outcome of the method employed in this work was evaluated through scatter diagrams and time history-based comparisons as well as through derivation of error statistics of R, RMSE and MAE. Figure 5a shows the scatter of numerically predicted versus actual current (meridional) at the same time steps while Fig. 5b depicts the scatter of ANN-corrected current (meridional) over

Table 1 Comparison of numerical estimations with measurements

Site	Velocity (U)—zonal			Velocity (V)—meridional		
	R	RMSE (cm/s)	MAE (cm/s)	R	RMSE (cm/s)	MAE (cm/s)
1	0.47	23.21	17.94	0.09	22.62	18.18
2	0.25	20.91	15.29	0.04	16.42	10.69

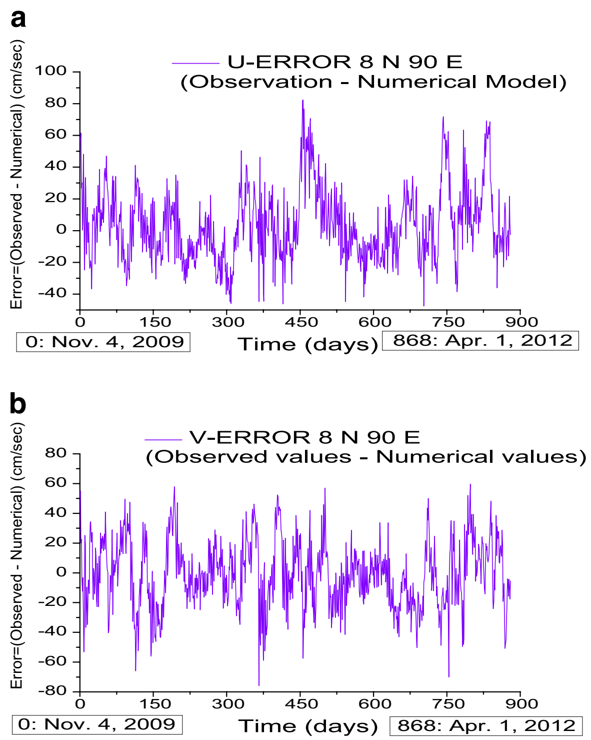

Fig. 4 An example of error time series at site: 1 for **a** u-component and **b** v-component

1-day ahead prediction. The corresponding time series-based comparison is presented in Fig. 5c.

The above diagrams qualitatively indicate that the procedure followed in this work has paid dividend in predicting current values.

An overall quantitative performance of the suggested approach of refining the numerical outcome over the testing period is given in Table 2. It may be seen from this Table that while the raw numerical estimation is associated with low R and high RMSE and MAE the predictions are relatively much satisfactory up to 5 days in future. For the U (zonal) component the latter resulted in producing current values with a mean error of 10.70 cm/s and root mean square error of 13.40 cm/s for the next day forecast. These values however increased to 15.79 and 19.75 cm/s for the 5-day ahead prediction. For the V (meridional) component the adopted procedure resulted in producing current values with mean error of 11.35 cm/s and root mean square error of 14.70 cm/s for the next day forecast. These values however increased to 16.25 and 20.61 cm/s for the 5-day ahead prediction.

It may be noticed that although the method's performance reduced with lead time the predictions were fairly good till five time steps ahead. The ANN looks for some unknown hidden pattern in the occurrence of preceding values rather than a serial correlation between them and hence the study of the serial correlation (normally based on the assumption of linearity of relationships) was avoided in this work. Although the effect of adding the error predicted by an ANN reduced with lead time, probably due to the difficulty in recognizing longer patterns by neural networks, the predictions were fairly good till five time steps ahead. Predictions beyond this were not so successful and RMSE and MAE reached the same level as raw numerical estimates thereafter. This could be because of the capability of the given network to manage data of certain sample size.

It is however observed that the improvement was different across the two current components. Better modification was seen for the V- or meridional component which was relatively better predicted in the very beginning by the numerical model.

When the performance of the 'error' network' (or ANN operating on the errors) was evaluated with R, RMSE and MAE, it was found that as expected RMSE and MAE remain same as that of the RMSE and MAE given in Table 2; however the R value changed differently, as 0.80, 0.71, 0.70, 0.63, and, 0.57 with the change in the lead time from 1 to 5 days. This was the case with the U-component. With respect to the V-component the corresponding changes in R were 0.76, 0.66, 0.62, 0.51, and, 0.44. This change in R however does not appear to be significantly larger and hence the error network seemed to have performed mostly similar to the combined numerical-ANN scheme.

The above procedure was further implemented at another site to see if the approach succeeds similarly when the location changes.

Site 2

For this location and over the testing duration Fig. 6a shows the scatter of numerically predicted versus actual current (zonal) at the same time steps, Fig. 6b that of the ANN-corrected current (zonal) while Fig. 6c presents a time series based comparison for the same data (as in Fig. 6a, c over a 3-day ahead prediction. These figures clearly indicate that the procedure of correcting the numerical outcome followed in this work has been very useful in predicting current values at this site also.

For the entire testing period an overall quantitative performance of the suggested approach of refining the numerical outcome is given in Table 3. It shows that while the original numerical estimation has low R and high RMSE and MAE (more so for the V- component) the revised predictions were much satisfactory up to 5 days in future. For the U (zonal) component the error addition resulted in producing current values with a mean error of 6.30 cm/s and root mean square error of 8.00 cm/s for

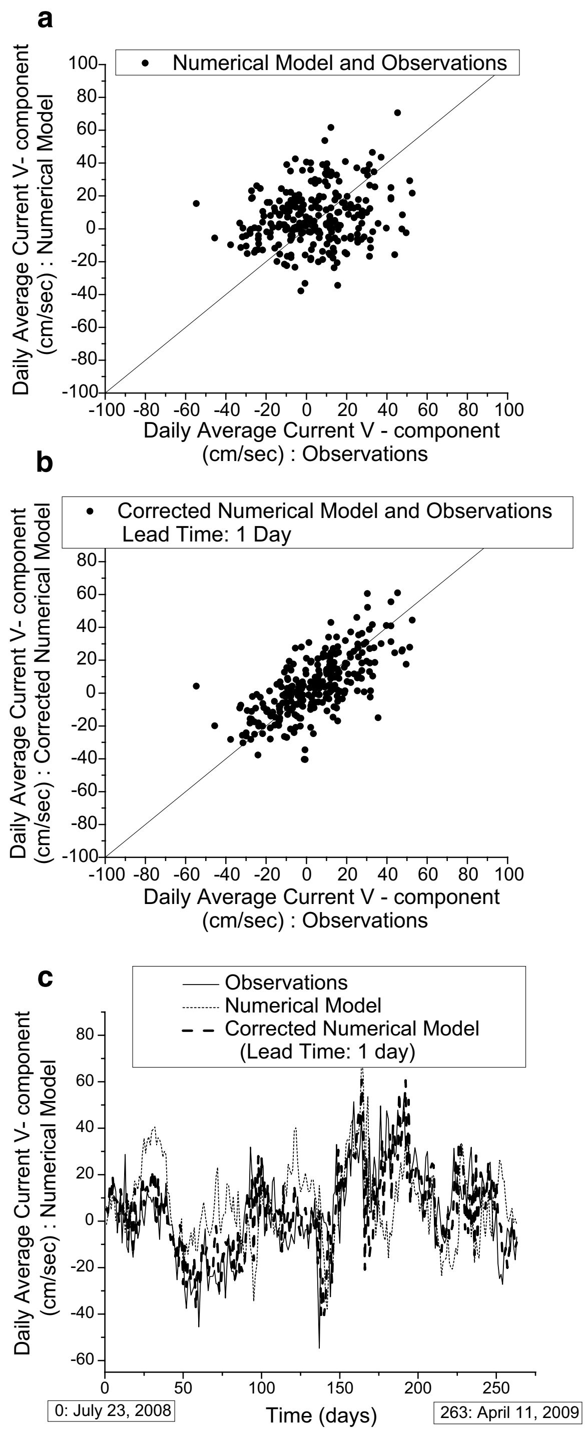

Fig. 5 **a** Scatter of numerical versus actual current (meridional) at the same time step, **b** scatter of corrected numerical versus actual current (meridional) for a 1-day ahead prediction, **c** time series of raw numerical, corrected numerical as well as actual current (meridional) all at site 1 for testing period

Table 2 ANN-corrected numerical current prediction at site: 1 (testing period)

	Velocity (U)			Velocity (V)		
	R	RMSE (cm/s)	MAE (cm/s)	R	RMSE (cm/s)	MAE (cm/s)
Numerical vs. observations	0.50	25.28	19.00	0.22	22.98	18.99
	Velocity (U)			**Velocity (V)**		
	R	**RMSE (cm/s)**	**MAE (cm/s)**	**R**	**RMSE (cm/s)**	**MAE (cm/s)**
Lead time (days)	Corrected prediction × observations					
1	0.80	13.40	10.70	0.70	14.70	11.35
2	0.71	16.08	12.90	0.60	17.16	13.09
3	0.70	16.60	13.23	0.56	18.01	13.98
4	0.63	18.21	14.72	0.48	19.74	15.68
5	0.57	19.75	15.79	0.44	20.61	16.25

the next day forecast. These values however increased to 9.86 and 12.34 cm/s for the 5-day ahead prediction. For the V (meridional) component the error assimilation resulted in producing current values with mean error of 8.21 cm/s and root mean square error of 11.73 cm/s for the next day forecast. These values however increased to 14.63 and 19.63 cm/s for the 5-day ahead prediction.

Similar to site 1 although the effect of data assimilation reduced with lead time the predictions were fairly good till five time steps ahead. The improvement was different across both current components. A high amount of modification was seen in the V- or meridional component which was more poorly predicted in the very beginning.

If we see Fig. 2a, b and further Tables 2 and 3 we may find that the performance at site 2 was relatively better than the one at site 1. The exact reason behind this is difficult to state in view of involvement of only two locations; however a rough guess is that this could be because the current flow at site 2 had lesser directional spread and further the initial numerical predictions (the u-component) there had better accuracy to begin with, which might have made the ANN based modelling easier.

At this site 2, when the performance of the 'error' network was evaluated with R, RMSE and MAE, it was found that, as expected, RMSE and MAE remained same as that of RMSE and MAE given in Table 3; however the R value changed differently, as 0.86, 0.85, 0.76, 0.73, and 0.67 for the U-component with the change in the lead time from 1 to 5 days. Thus unlike the earlier site 1, here

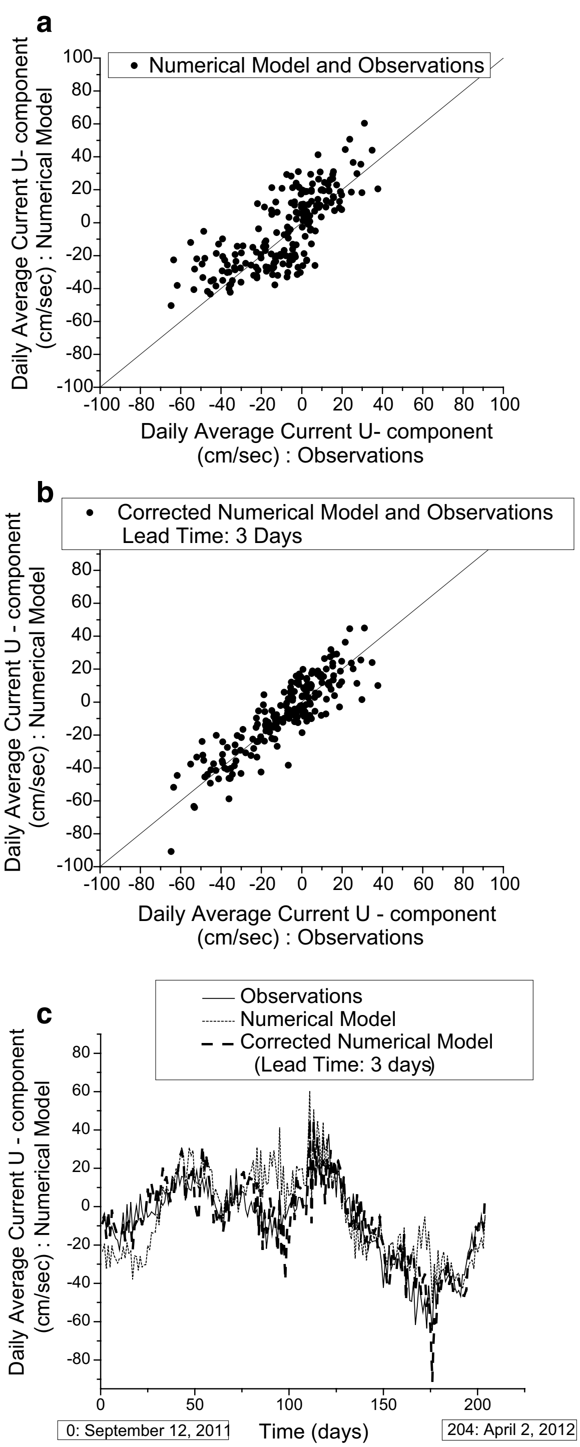

Fig. 6 **a** Scatter of numerical versus actual current (zonal) at the same time step, **b** scatter of corrected numerical versus actual current (zonal) for a 3-days ahead prediction, **c** time series of raw numerical, corrected numerical as well as actual current (zonal) all at site 2 for testing period

Table 3 ANN-corrected numerical current prediction at site: 2 (testing period)

	Velocity (U)			Velocity (V)		
	R	RMSE (cm/s)	MAE (cm/s)	R	RMSE (cm/s)	MAE (cm/s)
Numerical v/s observations	0.75	15.86	12.67	−0.01	26.99	21.54
	Velocity (U)			**Velocity (V)**		
	R	**RMSE (cm/s)**	**MAE (cm/s)**	**R**	**RMSE (cm/s)**	**MAE (cm/s)**
Lead time (days)	Corrected prediction × observations					
1	0.93	8.00	6.30	0.77	11.73	8.21
2	0.92	8.24	6.67	0.68	13.56	9.67
3	0.88	10.40	8.21	0.59	16.41	11.87
4	0.87	11.15	8.88	0.50	16.88	12.70
5	0.85	12.34	9.86	0.37	19.63	14.63

at site 2 the correlation between the realized and target errors was comparatively somewhat less. However, with respect to the V-component such correlation was high (R values being 0.90, 0.87, 0.77, 0.79, and 0.70, over the five lead times). The performance of the error network vis-à-vis that of the resultant numerical-neural prediction thus appears to be changing with the site as well as with the given current component.

As discussed in Saha et al. (2015) most of the physics-based or data-driven methods employed in the past suffered either from low accuracy at extremes or from highly unequal accuracy levels across the meridional and zonal components of current. As seen from our results our approach is free from these defects.

While the Figs. 5 and 6; Tables 2 and 3, referred to above, give an idea of the performance of the suggested model with respect to the current magnitudes, the same in respect of current vectors is exemplified in Figs. 7 and 8. These Figures pertain to the testing period and at sites 1 and 2, respectively. Figures 7a and 8a show the current rose diagram as observed while Figs. 7b and 8b give the same as per the corrected numerical procedure. It can be seen from these figures that there is a good resemblance between the two rose diagrams of the observed and predicted currents.

Stand-alone neural networks

Apart from the numerical-ANN combination discussed above an attempt was made to see if ANNs can learn the numerical output and reproduce it for future. This

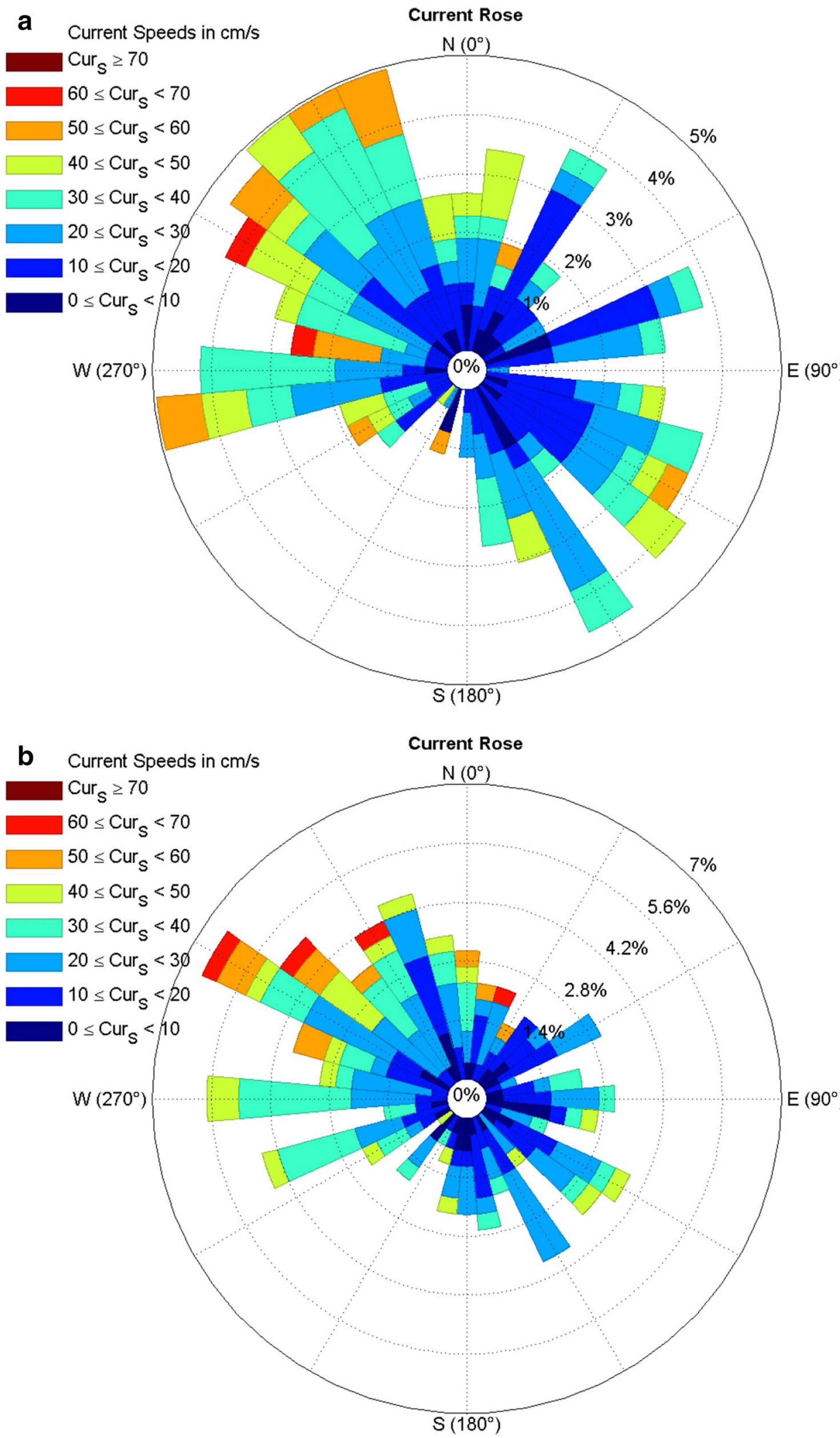

Fig. 7 Current rose diagrams over the testing period **a** observations, **b** corrected numerical method; site 1; lead time: 1 day

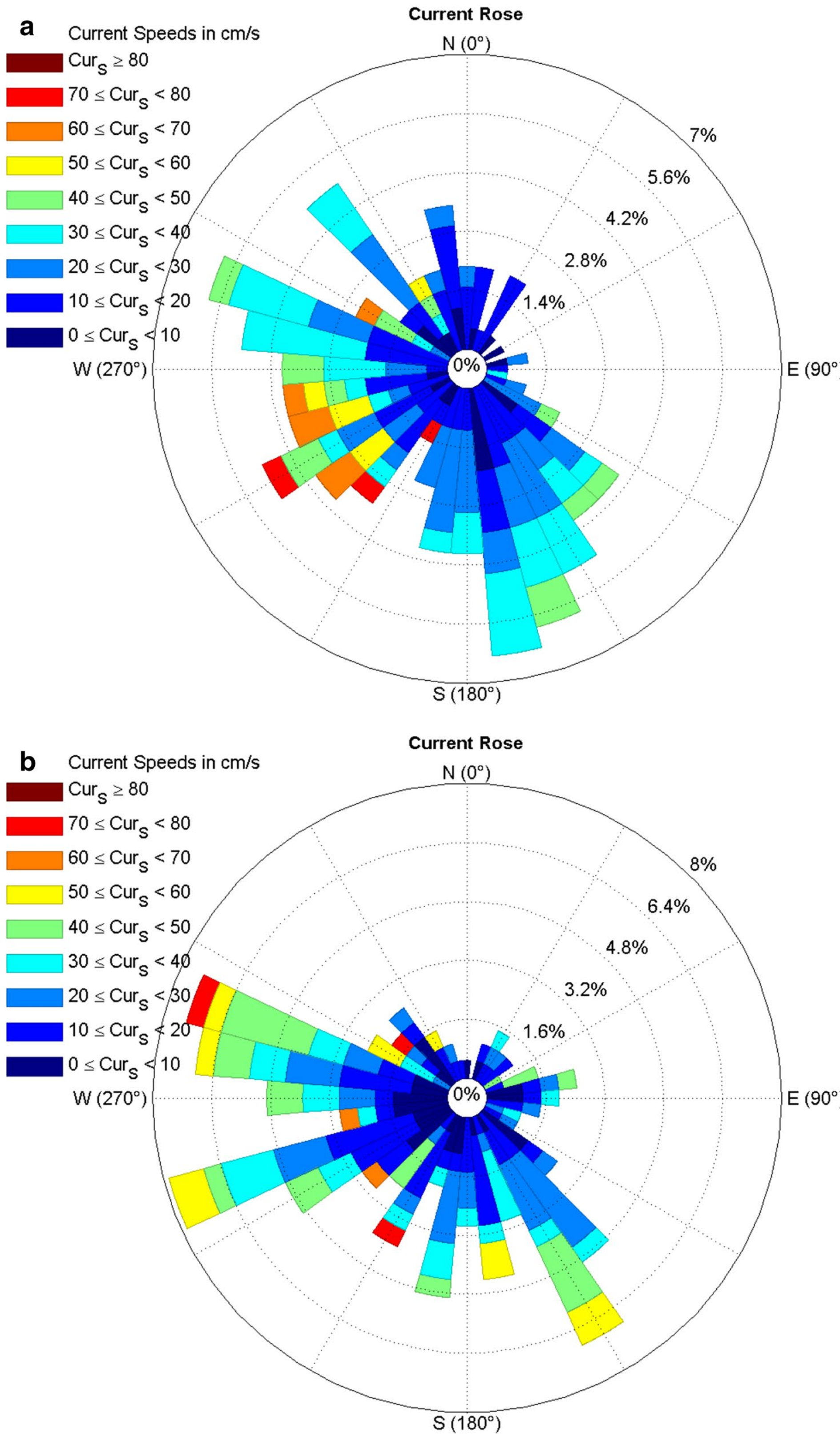

Fig. 8 Current rose diagrams over the testing period **a** observations, **b** corrected numerical method; site 2; lead time: 3 days

Table 4 Performance of the stand-alone models (site 1)

	Velocity (U)			Velocity (V)		
	R	RMSE (cm/s)	MAE (cm/s)	R	RMSE (cm/s)	MAE (cm/s)
Lead time (days)	Prediction of numerical output with ANN					
1	0.93	9.38	6.87	0.86	9.00	6.84
2	0.87	13.07	9.92	0.73	11.87	9.26
3	0.86	13.98	10.66	0.67	12.81	10.00
4	0.84	14.87	11.58	0.58	14.17	11.16
5	0.82	15.89	12.54	0.48	15.21	12.00

Table 5 Performance of the stand-alone models (site 2)

	Velocity (U)			Velocity (V)		
	R	RMSE (cm/s)	MAE (cm/s)	R	RMSE (cm/s)	MAE (cm/s)
Lead time (days)	Prediction of numerical output with ANN					
1	0.91	9.37	7.11	0.81	10.63	7.94
2	0.91	9.64	7.20	0.81	11.94	9.24
3	0.88	11.22	8.72	0.72	12.42	8.85
4	0.86	11.85	9.18	0.68	13.46	10.00
5	0.84	12.99	10.22	0.65	13.95	10.15

consisted of developing stand-alone networks (with no error calculations involved) trained on the basis of past numerical estimations and enabling them to predict the meridional and zonal current components over next 5 days. Thus the purpose of this section is to see if stand alone ANN's are good enough in reproducing the numerical output without going through the rigorous numerical procedures in real time and without providing high amount of exogenous input. Such ANN's are trained in this work using outcome of the numerical method rather than actual observations in light of the fact that continuous current measurements at any given site may not be always available. In the end we find that such ANN's can provide satisfactory forecasts and can be used at engineering site offices or so where vast computational or data resources required to run the numerical models are not available.

The input to the stand alone ANN consisted of a segment of past values of the numerically evaluated current. The length of the segment (or the number of neurons in the input layer) was ascertained by experiments aimed at achieving the best performance. This was typically five. The output was the predicted current corresponding to the lead time under consideration. For each lead time separate networks were developed. The number of hidden nodes was selected through trials aimed at obtaining the best testing performance and this was typically 10. The training algorithm of resilient back-propagation referred to earlier involved the use of a momentum factor of 0.7 and learning rate of 0.9

The results of the above exercise in terms of the error statistics (for ANN predictions versus corresponding numerical values) are shown in Table 4 for site 1 and in Table 5 for site 2. It may be seen that although the performance was lower for the V-component (which were originally not well estimated by the numerical method) than the U-component and that it reduced with increasing lead times, still the R value was quite high and RMSE and MAE were fairly low over the prediction horizon of 5 days.

Thus the network can be seen as a computationally faster alternative to the numerical runs when prediction over multiple time steps in future is desired.

A look into Tables 4 and 5 indicates that in case of the stand alone ANN-based models the performance at both the sites was generally similar, as against the earlier case of ANN-corrected numerical predictions (in which case better predictions were seen at site 2). The stand alone models thus seem to be independent of the accuracy of the initial numerical predictions.

If we compare long lead time predictions of Tables 2 and 3 with corresponding Tables 4 and 5 we find that the stand alone networks exhibit better performance at higher lead times than the combined numerical-neural method. This indicates superiority of a data-driven approache in site-specific environment. The ANN learns with more degrees of freedom than the numerical scheme and thus produces better results at higher lead times.

Limitations

Although the numerical methods in general should work well in an open ocean location compared to a nearshore coastal one where the effect of complex bottom topography or shoreline geometry might dominate, our analysis presented herein indicates that this may not always happen. Thus the station-specific numerical outcome even if it is made at an open sea location may need post-processing, as done in this study. However it is clarified that the reported work is more like proof-of-concept study and if it is to be extended for bias correction of the entire numerical outcome then techniques such as ensemble error covariance as suggested as in Sannasiraj et al. (2006) and Sannasiraj (2012) may be adopted. These methods in turn need current measurements at multiple locations for their application. If such observed information is not available then we have to go for other methods of data assimilation, namely, updating input or state variables or model parameters (Sannasiraj et al. 2006).

Conclusions

The adopted method of combining the numerical current estimation and its errors predicted by an artificial neural network resulted in prediction of the two components of ocean currents with good accuracy at both locations considered in this work. Predictions over the entire range of values including the higher ones were satisfactory.

Both meridional as well as zonal components were well predicted. However more accuracy was gained by the suggested procedure when the original numerical estimations themselves were relatively better.

Stand-alone neural networks trained on the outcome of a numerical model were found to make current predictions with high fidelity with the original numerical outcome.

Authors' contributions

All authors contributed to design, analysis, data compilation, and, interpretation of results. All authors read and approved the final manuscript.

Author details

[1] Department of Civil Engineering, Indian Institute of Technology Bombay, Mumbai, India. [2] Indian National Centre for Ocean Information Services, Hyderabad, India. [3] Nuclear Research Board, Bhabha Atomic Research Centre, Mumbai, India.

Acknowledgements

The authors are grateful to TAO Project Office of NOAA/PMEL for making available on website the buoy data from Indian Ocean for this study.

Authors also thank the anonymous reviewers who significantly enhanced the interpretation of our results.

Competing interests

The authors declare that they have no competing interests.

Received: 4 December 2015 Accepted: 20 January 2016
Published online: 01 February 2016

References

Bolanos R, Sorensen JVT, Benetazzo A, Carniel S, Sclavo M (2014) Modelling ocean currents in the northern Adriatic Sea. Cont Shelf Res 87(2014):54–72

Charhate SB, Deo MC, Sanil Kumar V (2007) Soft and hard computing approaches for real time prediction of currents in a tide dominated area. J Eng Marit Environ, Proceedings of the Institution of Mechanical Engineers, London, Part M, 221/2007, p 147–163

Chelton DB, Schlax MG, Samelson RM (2011) Global observations of nonlinear mesoscale eddies. Prog Oceanogr 91:167–216

Farrara JD, Chao Y, Li Z, Wang X, Jin X, Zhang H, Li P, Vu Q, Olsson PQ, Schoch GC, Halverson M, Moline MA, Ohlmann C, Johnson M, McWilliams JC, Colas FA (2013) A data-assimilative ocean forecasting system for the Prince William sound and an evaluation of its performance during sound Predictions 2009. Cont Shelf Res 63(2013):S193–S208

Fu L-L (2007) Intraseasonal variability of the equatorial Indian Ocean observed from sea surface height, wind, and temperature data. J Phys Oceanogr 37:188–202

Hermes JC, Reason CJC (2008) Annual cycle of the South Indian Ocean (Seychelles-Chagos) thermocline ridge in a regional ocean model. J Geophys Res 113:C04035. doi:10.1029/2007JC004363

Iskandar I, McPhaden M (2011) Dynamics of wind-forced intraseasonal zonal current variations in the equatorial Indian Ocean. J Geophys Res 116:C06019. doi:10.1029/2010JC006864

Jain P, Deo MC (2006) Neural networks in ocean engineering. Int J Ships Offshore Struct Taylor Francis 1(1):25–35

Joseph S, Ravichandran M (2013) "Validation of 0.25 × 0.25 Indian Ocean HYCOM", INCOIS Report. http://www.incois.gov.in/documents/hycom/hycom_0.25x0.25_tech_rep.pdf. Accessed 1 Aug 2013

Karri RR, Wang X, Gerritsen H (2014) Ensemble based prediction of water levels and residual currents in Singapore regional waters for operational forecasting. Environ Model Softw 54(2014):24–38

Kowalik Z, Marchenko A, Brazhinov D, Marchenko N (2015) Tidal currents in the western Svalbard Fjords. Oceanologia 57:318–327

Londhe S, Panchang V (2006) One day wave forecasts based on artificial neural networks. J Atmos Ocean Technol 23(11):1593–1603

Makarynskyy O (2004) Improving wave predictions with artificial neural networks. Ocean Eng 31(2004):709–724

Masumoto Y, Meyers G (1998) Forced Rossby waves in the southern tropical Indian Ocean. J Geophys Res 103(C12):27589–27602

McPhaden MJ, Meyers G, Ando K, Masumoto Y, Murty VSN, Ravichandran M, Syamsudin F, Vialard J, Yu L, Yu W (2009) Supplement to "RAMA: the research moored array for African—Asian—Australian monsoon analysis and prediction. Bull Amer Meteor Soc 90:459–480. doi:10.1175/2008BAMS2608.2 **(ES5–ES8)**

Rahaman H, Ravichandran M, Sengupta D, Harrison MJ, Griffies SM (2014) Development of a regional model for the North Indian Ocean. Ocean Model 75(2014):1–19

Saha D, Deo MC, Bhargava K (2015) Prediction of ocean currents with artificial neural networks. ISH J Hydraul Eng 21(1):14–27

Sannasiraj SA (2012) Data assimilation for wave forecasting. Proceedings, "Hydro-2012", conference, IIT Bombay, Mumbai, India December 7–8, 2012, 119–130

Sannasiraj SA, Babovic V, Chan ES (2006) Wave data assimilation using ensemble error covariance's for operational wave forecast. Ocean Model 14(2006):102–121
Schimdt A, Gangopadhyay A (2013) An operational ocean circulation prediction system for the western North Atlantic: hindcasting during July–September of 2006. Cont Shelf Res 63(2013):S177–S192
Sivakumar B., and Berndtsson R., (2010): "Advances in data-based approaches for hydrologic modeling and forecasting", 2010 Edition, World Scientific, (2010)
Wang Y, Wei Z, Lian Z, Yang Y (2015) Development of an ocean current forecast system for the South China Sea. Aquatic Procedia 3(2015):157–164
Wasserman PD (1993) Advanced methods in neural computing. Van Nostrand Reinhold, New York
Wilby RL, Wigley TML (1997) Downscaling general circulation model output: a review of methods and limitations. Prog Phys Oceanogr 21(4):530–548
Wu KK (1994) Neural networks and simulation methods. Marcel Decker, New York